https://doi.org/10.5194/gmd-2020-111
Preprint. Discussion started: 30 April 2020

Geoscientific Model Development
Discussions
Open Access

Introducing LAB60: A 1/60° NEMO 3.6 numerical simulation of the Labrador Sea

Clark Pennelly[1*] and Paul G. Myers[1]

[1]1-26 Earth Sciences Building, University of Alberta, Edmonton, Alberta, Canada, T6G 2E3

[*]*Correspondence to*: Clark Pennelly (pennelly@ualberta.ca)

Abstract

A high-resolution coupled ocean-sea ice model is set up within the Labrador Sea. With a horizontal resolution of 1/60°, this simulation is capable of resolving the multitude of eddies which transport heat and freshwater into the interior of the Labrador Sea. The transport of these fluxes strongly governs the overall stratification, deep convection, and subsequent production of Labrador Sea Water. We implement nested domains within our regional configuration to reduce computational costs, allowing for a simulation that spans over 10 years. Three passive tracers are also included: Greenland runoff, Labrador Sea Water produced during convection, and Irminger Water which enters the Labrador Sea along Greenland. We describe the configuration setup and compare against similarly forced lower-resolution simulations to better describe how horizontal resolution impacts the Labrador Sea.

Introduction

The Labrador Sea, between Canada and Greenland, plays a crucial role in the climate system. Situated between the Canadian Arctic and the North Atlantic, multiple current systems influence this deep basin. Cold and fresh Arctic water flows south through Fram Strait along Greenland (de Steur et al., 2018), producing the East Greenland Current (EGC). The EGC flows to the southern tip of Greenland, merging with warm and salty Irminger Water before flowing northwards along the western coast (Fratantoni and Pickart, 2007). Together, these combine to become the West Greenland Current (WGC) which flows cyclonically around the Labrador Sea as well as into Baffin Bay. Significant amounts of freshwater are supplied to the current system from both Davis (Cuny et al., 2005, Curry et al., 2011, Curry et al., 2014) and Hudson Strait (Straneo and Saucier, 2008) as it travels around the Labrador Sea. The current system, now

https://doi.org/10.5194/gmd-2020-111
Preprint. Discussion started: 30 April 2020

Geoscientific Model Development
Discussions

called the Labrador Current (Lazier and Wright, 1993), travels southwards along the eastern coast of North America, leaving the Labrador Sea.

Numerous eddies are generated throughout the Labrador Sea, both from high lateral density gradients which exist during the convection season (Frajka-Wiliams et al., 2014) as well as from baroclinic and barotropic instabilities that occur along the shelf break (Chanut et al., 2008; Gelderloos et al., 2011). The continental slope along the west coast of Greenland has a pronounced change in topography that induces instability of the current system, generating eddies (de Jong et al., 2016). These eddies, known as Irminger Rings, contain a significant amount of freshwater at the surface as well as subsurface heat. These Irminger Rings (15-30km radius) typically travel southwestwards into the interior of the Labrador Sea and have a lifespan of up to two years (Lilly et al., 2003). Eddies generated along the Labrador Coast also contain a significant amount of freshwater (Schmidt and Send, 2007; McGeehan and Maslowski, 2011; Pennelly et al., 2019). Regardless of where they are produced, boundary current eddies export their properties towards the centre of the basin, influencing the deep convection which occurs.

Only a few regions around the world experience deep convection. This includes the Ross and Weddell Sea near Antarctica (Gordon et al., 2007; Whitworth and Orsi, 2006), the Mediterranean Sea (Marshall and Schott, 1999; Brossier et al., 2017), and the North Atlantic containing the Nordic Seas (Hansen and Østerhus, 2000), Irminger Sea (Bacon et al., 2003), and Labrador Sea (Lazier et al., 2002; Yashayaev and Loder, 2016). The reason so few places exist is the stringent criteria to produce deep convection: weak stratification which is strongly influenced by cyclonic circulation, and intense air-sea buoyancy loss (Lab Sea Group, 1998; Marshall and Schott, 1999). Cyclonic circulation and the lateral input of salty Irminger Water helps keep the Labrador Sea weakly stratified. Furthermore, the Labrador Sea experiences strong heat loss during the winter period due to the very cold mid-latitude cyclones which frequent the region (Schulze et al., 2016). The overlying cold and relatively drier air forces a significant flux of heat from the ocean to the atmosphere. This loss of heat promotes the surface layer to increase in density, overturning the weakly stratified water column such that the mixed layer can exceed 2000m in depth (Yashayaev, 2007), producing a thick, uniform water mass known as Labrador Sea Water (LSW)

https://doi.org/10.5194/gmd-2020-111
Preprint. Discussion started: 30 April 2020

Once the convective winter ends, the Labrador Sea quickly restratifies itself, primarily due to large horizontal density gradients as a result of the deep convection period (Frajka-Williams et al., 2014). While this quick restratification process takes a few months, the Labrador Sea is always receiving buoyant water from the boundary currents, providing both cold and fresh surface water as well as warm salty subsurface water (Straneo, 2006). While both the Labrador and West Greenland Current supply buoyant eddies towards the interior of the Labrador Sea, research suggests that the Labrador Coast supplies a smaller but significant amount whereas the West Greenland Current has a much larger impact (Myers, 2005; Pennelly et al., 2019).

The product of deep convection in this region is exported throughout the North Atlantic as well as southwards within the Deep Western Boundary Current (Kieke et al., 2009). While LSW is the lightest component within the Deep Western Boundary Current, it is one of the water masses which make up the lower limb of the Atlantic Meridional Overturning Circulation (AMOC). As the overturning circulation transports a significant amount of heat and dissolved gasses between the equator and polar regions, changes in the amount of deepwater produced can influence the overturning circulation and ultimately the climate (Bryden et al., 2005). With polar amplification causing additional freshwater to enter the EGC/WGC, the Labrador Sea is experiencing an increase in freshwater that can be capable of capping convection and preventing LSW from being formed, ultimately reducing the AMOC strength (Böning et al., 2016).

While satellite altimetry provides a wealth of information, hydrographic cruises within the Labrador Sea are often limited to the restratification period when the Labrador Sea is more hospitable for scientific operations. Even ARGO floats, autonomous drifting profilers which sample down to 2000m, while their abundance has been increasing since 2002, still lack coverage within the Labrador Sea which sometimes encounters deep convection below their sampling depth. Numerical modelling is a useful tool to explore this data-sparse region, though it has its limits. Simulations within the Labrador Sea often experience a drift in model data, producing a Labrador Sea which slowly increases in salinity, and thus density (Treguier et al., 2005; Rattan et al., 2010). Coarse-resolution simulations suffer even further, often producing a

https://doi.org/10.5194/gmd-2020-111
Preprint. Discussion started: 30 April 2020

Geoscientific Model Development Discussions

significantly larger spatial extent of deep convection (Courtois et al., 2017), primarily as a result of not resolving important small-scale features including eddies. These eddies supply the Labrador Sea with significant heat and freshwater fluxes, both which strongly impact the stratification, convection, and production of deep water. While increasing the horizontal resolution helps in the production of eddies and their important fluxes into the interior of the Labrador Sea, numerical drift still is present within high-resolution simulations, albeit reduced in severity (Marzocchi et al., 2015).

Numerous high resolution simulations have been carried out within the North Atlantic. VIKING20X (Rieck et al., 2019), and its predecessor VIKING20, are global 1/4° simulations which have a high-resolution 1/20° nest. VIKING20X is a multi-decade simulation which is capable of resolving eddies within the Labrador Sea. Higher-resolution simulations such as a 1/50° HYCOM (Chassignet and Xu, 2017), the 1/60° NATL60 (Fresnay et al., 2018), and eNATL60 (Le Sommer et al., in prep) provide great insights on the importance of resolving eddies. However, computational expense with such high-resolution simulations is very high, both in computer time and operational costs. This often forces higher resolution simulations to have a reduced length, perhaps only a few years. The Labrador Sea experiences variability at the decadal scale (Fischer et al., 2010) and such short simulations may completely miss any connection between Labrador Sea Water production and changes in the Atlantic Meridional Overturning Circulation. As such, any high resolution simulations which are capable of resolving the fine scale features within the Labrador Sea should be carried out for over 10 years to further understand the climate system. Resolving the full North Atlantic at high resolution (1/60°) and carrying out a simulation for longer than 10 years would currently be extremely expensive. However, one can incorporate nested domains to increase horizontal resolution with a relatively minor increase in computing power.

To simulate the Labrador Sea as accurately as possible, we set up a complex numerical configuration which achieves very high resolution within the Labrador Sea while keeping computing costs low such that we produce over one decade of data. The high resolution allows for explicit representation of eddies which are crucial to controlling the stratification within the region. We will first describe the model configuration in detail, and then compare against

https://doi.org/10.5194/gmd-2020-111
Preprint. Discussion started: 30 April 2020

Geoscientific Model Development
Discussions

similarly-forced lower-resolution simulations to understand how changes in horizontal resolution impacts model results in the Labrador Sea.

Methods

The numerical model used for our high-resolution simulation is the Nucleus for European Modelling of the Ocean (NEMO; Madec, 2008), version 3.6, which is coupled to a sea-ice model, LIM2 (Fichefet and Maqueda, 1997). The 1/4° Arctic Northern Hemisphere Atlantic configuration (ANHA4; Fig 1a) is used and includes a nest via the Adaptive Grid Refinement in FORTRAN package (AGRIF; Debreu et al., 2008). The parent domain's nest uses a spatial and temporal refinement factor of three, bringing resolution to 1/12° in the North Atlantic Sub Polar Gyre domain (SPG12; Fig 1b). The SPG12 configuration has been evaluated before by investigating how model resolution influences Labrador Sea Water formation (Garcia-Quintana et al., 2019) as well as eddy formation and eddy fluxes in the North Atlantic Current (Müller et al., 2017; Müller et al., 2019). Another nest is implemented within SPG12, using a spatial and temporal refinement of five, increasing the horizontal resolution to 1/60° within the Labrador Sea (LAB60; Fig 1c). All nests allow two-way communication such that the parent domain supplies boundary conditions while the daughter domain returns interpolated values to all associated parent grid points. While all domains have different horizontal grid resolution, they share the same vertical grid which is set to 75 geopotential levels using partial steps (Fig. 1d). While this simulation involves three domains, we refer to the entire simulation as LAB60 and primarily only discuss what occurs within the 1/60° nest.

All domains used a total variance dissipation scheme (Zalesak, 1979) to calculate horizontal advection. Lateral diffusion used a Laplacian operator while lateral momentum mixing used a bi-Laplacian operator. As some model parameters are grid-scale dependent, Table 1 displays these settings. As lateral boundary conditions have been shown to be very important at producing Irminger Rings in high resolution simulations (Rieck et al. 2019), we used no-slip lateral boundary conditions within the LAB60 domain while the other domains had free-slip conditions. Model mixed layer depths were calculated via the vertical gradient in temperature and salinity (Holte and Talley, 2009) as opposed to the usual NEMO method of a

https://doi.org/10.5194/gmd-2020-111
Preprint. Discussion started: 30 April 2020

0.01 kg m^{-3} change in potential density between the surface and the bottom of the mixed layer; the latter method can produce deeper mixed layers than observations suggest (Courtois et al., 2017). Settings not listed in Table 1 indicate that all domains have an identical value or option; some of these important settings are shown in Table 2.

Model bathymetry was interpolated from the 1/60° ETOPO GEBCO dataset (Amante and Eakins, 2009) to each domain's grid, though bathymetric smoothing between domains occurred along boundary nests. All domains were initialized from GLORYS1v1 (Ferry et al., 2009), a global reanalysis ocean simulation, at the beginning of 2002. Open boundary conditions from the same dataset are applied at monthly intervals to the parent ANHA4 domain. Runoff was supplied via Dai et al. (2009) while we also included Greenland runoff as estimated from a surface mass-balance model (Bamber et al., 2012). Without an iceberg model functioning with the AGRIF software, we treated all solid runoff as a liquid, thus capturing the full freshwater mass at the cost of accuracy in the spatial and temporal placement of freshwater emitted from icebergs. See Marson et al. (2018) about details regarding numerical modelling of Greenland's icebergs and how their freshwater release impacts the North Atlantic.

Atmospheric forcing including precipitation, shortwave radiation, downward longwave radiation, 2 meter specific humidity, 2 meter temperature, 10 meter meridional and 10 meter zonal winds originally were supplied from the Canadian Meteorological Centre's Global Deterministic Prediction System's Reforecast product (CGRF; Smith et al., 2014). While high in temporal (hourly) and spatial resolution (33 km in the Labrador Sea), we found the air-sea fluxes were slightly too weak to sustain deep convection after 2010. Rather than start completely over, we restarted the simulation from 2007 when LAB60's mixed layer was still similar to observations. Starting on 1 Jan 2007, we used the DRAKKAR Forcing Set 5.2 (DFS; Dussin et al., 2016). This forcing set has a spatial resolution of roughly 45 km in the Labrador Sea. Our own analysis of the CGRF data showed a long-term heat loss of 35 W m^{-2} from the interior Labrador Sea, while DFS removed 43 W m^{-2}. Increasing the horizontal resolution likely increased the horizontal buoyancy fluxes and rendered the CGRF's air-sea heat loss, which were appropriate in our ANHA4 and ANHA12 configuration, inadequate. The decision to swap to DFS was based on its greater heat loss, promoting a better mixed layer depth throughout the

https://doi.org/10.5194/gmd-2020-111
Preprint. Discussion started: 30 April 2020

Geoscientific Model Development Discussions
Open Access
EGU

Labrador Sea, though a different forcing product will eventually be needed as DFS does not currently extend past 2017. Supplemental Fig. 1 identifies the mixed layer depth between the LAB60 simulation forced by CGRF (LAB60-CGRF), when forced with CGRF through 2007 and then forced by DFS (LAB60-DFS), as well as what ARGO observations suggest. Note the lack of interannual variability and weak mixing within the post-2010 years of LAB60-CGRF when compared against the ARGO observations. While the DFS forcing promotes stronger heat loss from the ocean, these 2 forcing products have different resolution and data frequency: DFS's wind, temperature and humidity data have data every three hours while the precipitation and radiation data are daily. While we ran LAB60 with the CGRF forcing from 2002 through 2017, the remainder of this document will discuss the LAB60 simulation forced with DFS. This simulation (LAB60-DFS) is currently in the year 2011 at the time of this manuscript's submission.

While our internal testing showed that each passive tracer adds approximately 20% overhead to the simulation, three passive tracers were selected. Runoff from Greenland was included due to the importance of Greenland's freshwater contribution to changes within the Labrador Sea. Labrador Sea Water (σ>27.68 kg m^{-3}) produced annually within the mixed layer was included to identify the pathways which this water mass leaves its region of origin. Irminger Water (T> 3.5°C, S>34.88) that flows west past Cape Farwell was included as it provides a substantial amount of heat, and thus buoyancy, to the Labrador Sea, helping restratify the region. Figure 2 illustrates both the source regions as well as the tracer extent as of 1 Jan 2010. While these masses have been studied before in the past, there has been no attempt here to examine how they are represented at such resolution.

The LAB60 simulation originally started on the Graham cluster of Compute Canada. While other high-resolution simulations often use thousands of computer processors, our simulation could not run on more than 672 CPUs on this cluster as it would stall during domain construction. The years 2002-2007 were carried out on Graham, after which a new allocation on a different high performance Compute Canada cluster, Niagara, became available to us. The LAB60 simulation on Niagara did not suffer from the same issue as it did on Graham and we were able to use many more processors. Initial testing found substantial increase in simulation

https://doi.org/10.5194/gmd-2020-111
Preprint. Discussion started: 30 April 2020

length when the number of CPUs was increased from 672 to 3000, though tests using 4000 CPUs showed no further improvement. Thus, we carried out the remainder of the LAB60 simulation with 3000 CPUs. Each job submission required around 22 hours to carry out, providing 40 days of model output. The real time to finish each 40 day submission naturally varied across the year, primarily in response to seasonal sea ice.

From interpolating the 1/12° GLORYS1v1 data onto the 1/60° nest, we learned that the model simulation would quickly go unstable without a gradual spin-up period. The spin-up process we used was to set the LAB60 nest to have the same eddy viscosity and diffusivity values as the SPG12 nest while keeping the timestep low. We gradually raised the timestep and reduced the viscosity and diffusivity values over the first year (year 2002) to what is within Table 1. Other than also increasing the timestep to stay in line with LAB60, no other values were changed across the coarser ANHA4 and SPG12 domains. To allow LAB60 to adjust to the final settings, we consider the 2003 year to be part of the spin-up phase. All results will be presented from the start of 2004 through the end of 2010- the last year completed with DFS forcing at the time of this writing.

Model Simulation Results

To understand some large differences gained by resolving the Labrador Sea at 1/60°, we compare the output of our LAB60 simulation with similarly forced ANHA simulations at both 1/4° (ANHA4) and 1/12° (ANHA12). Looking at the large-scale circulation of the Labrador Sea (Fig. 3), we note differences between the configurations and observations. All simulations have greater speed within the West Greenland Current and Labrador Current as altimetry observations suggest slower speeds here. Both the ANHA4 and ANHA12 configuration have greater values further up the western coast of Greenland, as well as connecting the West Greenland Current and the Labrador Current; features that do not occur in both LAB60 and observations. As LAB60 and observations have less average speed occurring within these boundary currents, we suspect that all configurations have some large differences in eddy activity, particularly along these shelf breaks.

https://doi.org/10.5194/gmd-2020-111
Preprint. Discussion started: 30 April 2020

Geoscientific Model Development Discussions
Open Access EGU

Examination of the eddy kinetic energy as computed from geostrophic velocities (EKE: $0.5(\overline{U_g'^2} + \overline{V_g'^2})$, Fig. 4) shows clear differences between these simulations and the AVISO observations. Observations show high levels of EKE coming from the west Greenland coast as well as along the Labrador coast's shelf break. While the EKE coming from west Greenland enters the interior of the Labrador Sea, that which stems from the Labrador coast does not penetrate far into the interior. The ANHA4 simulation has lower levels of EKE everywhere other than the North Atlantic Current, though the west Greenland coast contains elevated values. The ANHA12 simulation shows improvement, having much higher EKE coming from west Greenland though the EKE does not quite enter the interior of the Labrador Sea but instead stays in the northern Labrador Sea. Furthermore, there is additional EKE along the Labrador shelf break compared against ANHA4. The LAB60 simulation shows further improvement as the EKE signature from the west Greenland coast now enters into the interior of the Labrador Sea, and also shows distinct EKE along the Labrador shelf break. While the EKE field produce by LAB60 has some differences compared to the AVISO observations, they match far better than the other low-resolution configurations.

The differences in the EKE field between these configurations identify that each simulation is resolving features of varying spatial scales. The ANHA4 simulation, with low EKE within the Labrador Sea, does not adequately resolve eddies in this region, as illustrated with a snapshot of model relative vorticity (Fig. 5). However, the larger scale meanders within the North Atlantic Current are visible. ANHA12 shows a greater degree of mesoscale features, though distinct eddies within the Labrador Sea are also not resolved. LAB60 resolves eddies along both the west coast of Greenland as well as the Labrador Coast. A supplemental video showing LAB60's relative vorticity is shown in Supplementary Video 1.

A few Irminger Rings are shown in Fig. 6, a snapshot in time from 17 Jan 2003. A newly spawned ring (Fig. 6c) show very strong surface speeds (Fig. 6a) while older eddies to the southwest have reduced speeds. A snapshot of convective energy (our Fig. 6b; see Holdsworth and Myers, 2015) shows that most of these eddies have substantially higher amounts compared to the background Labrador Sea, suggesting that the cool and fresh WGC water, as well as warm and salty Irminger Water keep these eddies strongly stratified. However, these eddies age within the Labrador Sea, and while a new eddy has strong stratification, an eddy which has evolved over many months (Fig. 6d) has weaker stratification. Older eddies may even have weaker stratification than the background Labrador Sea. Considering Irminger Rings can live up to 2 years, such an eddy experiencing 2 convective winter periods might experience enough buoyancy loss such that Labrador Sea Water is produced within an Irminger Ring.

These differences in resolving the mesoscale and sub-mesoscale processes within each simulation produced significant changes within the Labrador Sea as seen from modeled convective energy values as averaged from 2004-2010 (Fig. 7). Without resolving Irminger Rings and other eddies, the ANHA4 simulation's interior Labrador Sea lacks the buoyancy flux associated with these eddies and remains very weakly stratified across a wide region. The ANHA12 simulation partially resolves some mesoscale features and eddy fluxes from the Greenland coast which supplies buoyancy to the Northern Labrador Sea, and has higher convective energy values as a result. Furthermore, the spatial extent of the weakly stratified region has shrunk and resides primarily within the Labrador Sea, as opposed to ANHA4 which spills out of the basin. LAB60, fully capable of resolving buoyant Irminger Rings from the west coast of Greenland, has a much stronger degree of stratification in the interior region. A visible path of strong stratification is visible leaving this coastline, between the 2500 and 3000m isobath, consistent with the general path that simulated Irminger Rings take (Chanut et al., 2008). Supplemental Video 2 shows the convective energy of the LAB60 simulation from 2004 through the end of 2010.

With less convective energy, the ANHA4 simulation experiences weaker stratification in the Labrador Sea. The ANHA4 simulation experiences a deeper maximum mixed layer that also covers a larger spatial extent than ANHA12 or LAB60 (Fig. 8). However, the maximum mixed layer depth as simulated by ANHA4 and ANHA12 greatly exceed what observation suggest (Fig. 8d). ANHA12's additional EKE along the west coast of Greenland supplied additional buoyancy to the northern portion of the Labrador Sea, limiting the mixed depth between the 2000m and 3000m isobath. Not only did this move the region of maximum depth slightly south and offshore, the additional buoyancy reduced the spatial extent of the mixed layer. With higher EKE values further offshore, the LAB60 simulation further reduced the northern convective

https://doi.org/10.5194/gmd-2020-111
Preprint. Discussion started: 30 April 2020

Geoscientific Model Development
Discussions
Open Access
EGU

area, reduced the overall spatial extent of the mixed layer, and reduced the depth even further. LAB60's mixed layer is far more similar to what ARGO observations suggest. The evolution of LAB60's mixed layer depth is shown in supplemental video 3 from 2004 through the end of 2010.

After the mixed layer returns to the near-surface, a newly formed LSW mass is left behind. We explore the density, referenced to 1000 dbar, and thickness of this water mass in Fig. 9. We define the yearly maximum density of this water mass as the thickest depth where the density changes by 0.001 kg m^{-3}. The minimum density is defined to be 0.02 kg m^{-3} lighter. Linear interpolation occurs between years to allow for a gradual shift in density to prevent stair-stepping patterns from emerging. Large differences in both the density as well as the thickness are present between the simulations shown in Fig. 9. First, the ANHA4 and ANHA12 simulation both have similar density values of LSW, though the LAB60 simulation has this water mass being less dense. While the interannual variability matches fairly well across all configurations, the density values suggested by LAB60 match far closer to ARGO observations (32.34 to 32.36 kg m^{-3}; Yashauaev and Loder, 2016) during the same time period. We suspect the denser LSW formed by ANHA4 and ANHA12 is primarily attributed to the lack of buoyancy coming from Greenland. While similar air-sea heat losses should occur between the configurations, the weaker stratification of ANHA4 and ANHA12 indicate that deep mixing is easier to occur, producing not only a denser LSW layer, but also a thicker one. Yashayaev and Loder (2016) also investigated the thickness of LSW (their Fig. 7), and while our simulations do not quite capture the same interannual variability and amplitude suggested by ARGO profilers, LAB60 is far more accurate than the lower resolution configurations.

The three passive tracers implemented within the full LAB60 configuration (Fig. 2) show where Greenland runoff, Irminger Water, and Labrador Sea Water travel to. These tracers were selected because they either contain a significant amount of buoyant water compared to the Labrador Sea, or are produced via convection in the Labrador Sea. From this image on 1 Jan 2010, we see a large portion of Greenland's runoff (Fig. 2a) resides within Baffin Bay as well as along the Labrador Coast. However, some enters the interior 2000m and 3000m isobath from along the west coast of Greenland; individual Irminger Rings containing sufficient amounts of

https://doi.org/10.5194/gmd-2020-111
Preprint. Discussion started: 30 April 2020

this tracer are visible within the 3000m isobath. While a fair amount of the tracer ends up within the Labrador Current, most appears to leave the shelf-break system in the vicinity of Flemish Cap, travelling eastwards. Supplemental Video 4 shows this the evolution of this tracer from 2004 through the end of 2010.

Irminger Water (T>3.5°C, S> 34.88; Fig. 2b) which flows west past Cape Farwell, enters the interior Labrador Sea, though mainly within the 2000m and 3000m isobath. Similar as above, individual Irminger Rings are visible, containing a thicker amount of Irminger Water than the surrounding water. This water mass also flows along the Labrador Coast until it is in the vicinity of Flemish Cap. Supplemental Video 5 shows this the evolution of this tracer from 2004 through the end of 2010.

Our Labrador Sea Water tracer (Fig. 2c) is traced where the mixed layer produces water with a density above 1027.68 kg m^{-3} within the black contour identified in the figure. As this image was made at the start of the convection season, the current deep patch is a freshly made thick layer that reaches up to 800m deep. After forming, LSW spreads southwards along the Labrador shelfbreak as well as to the southeast. Supplemental Video 6 shows this the evolution of this tracer from 2004 through the end of 2010.

Discussion

We describe a 10+ year long, high-resolution simulation which achieves 1/60° horizontal resolution in the Labrador Sea via two nests inside a regional configuration, resolving sub-mesoscale processes which strongly impact the deep convection which occurs here. We show that lower resolution simulations fail to resolve these key processes that strongly control the production of Labrador Sea Water, an important water mass within the Atlantic Meridional Overturning Circulation. While the NATL60 and eNATL60 simulations were designed with the SWOT altimetry satellite mission in mind (NATL60 website: https://meom-group.github.io/swot-natl60/virtual-ocean.html), their integration period is a handful of years. LAB60, although covering a much smaller region, could be a valuable asset to many users who require a lengthy period of high-resolution model output. We also have included three passive tracers which are often excluded in simulations at this resolution. Our three passive tracers

https://doi.org/10.5194/gmd-2020-111
Preprint. Discussion started: 30 April 2020

Geoscientific Model Development Discussions

highlight regions where each water mass enters the interior region of the Labrador Sea, demonstrating the pathways of buoyant Greenland melt and Irminger water. Furthermore, we trace Labrador Sea Water which is formed during the convective winter period. Current research project using the LAB60 simulation are focused on the variability of the West Greenland Coastal Current, Labrador Sea Water production, and Irminger Ring's role in controlling stratification in the Labrador Sea. This lengthy high-resolution simulation with three passive tracers will provide valuable information for many numerical studies within the Labrador Sea for years to come.

Code and/or data availability

The FORTRAN code used to carry out the LAB60 simulation can be accessed from the NEMO version 3.6 repository (https://forge.ipsl.jussieu.fr/nemo/browser/NEMO/releases/release-3.6). A few FORTRAN files were modified to handle our passive tracers. The complete FORTRAN files as well as the CPP.keys, namelists, and associated files can be found on Zenodo (Pennelly, 2020). Initial and boundary conditions, atmospheric forcing, and numerical output were too large to host on a repository and instead are hosted on our lab's servers as well as the Compute Canada Niagara server. These data can be requested by emailing the corresponding author.

Author Contribution

PM designed the layout of the LAB60 configuration which included the region of interest, numerical length, and which forcing and initial conditions to supply, as well as supervised CP. CP produced the configuration, modified the FORTRAN code, set up the configuration on the high-performance computing systems, carried out the simulation, performed the analysis. The manuscript was prepared by CP with contributions by PM.

Acknowledgements

The authors would like to thank the NEMO development team as well as the DRAKKAR group for providing the model code and continuous guidance. We express our thanks to

https://doi.org/10.5194/gmd-2020-111
Preprint. Discussion started: 30 April 2020

Geoscientific Model Development Discussions

Westgrid and Compute Canada (http://www.computecanada.ca) for the computational resources to carry out our numerical simulations as well as archival of the experiments. We would like to thank Nathan Grivault for his help to migrate our configuration between computing clusters, as well as Charlene Feucher for her help with ARGO data. This work was supported by an NSERC Climate Change and Atmospheric Research Grant (Grant RGPCC 433898) as well as an NSERC Discovery Grant (Grant RGPIN 04357).

The authors declare that they have no conflict of interest.

References

Amante, C. and Eakins, B.W.: ETOPO1 1 Arc-minute global relief model: procedures data sources and analysis. NOAA Technical Memorandum NESDIS, NGDC-24 19, 2009.

Bacon, S., Gould, W.J., and Jia, Y.: Open-ocean convection in the Irminger Sea. Geophysical Research Letters, 30(5), 2003.

Bamber, J., van den Broeke, M., Ettema, J., Lenaerts, J., and Rignot, E.: Recent large increases in freshwater fluxes from Greenland into the North Atlantic. Geophysical Research Letters, 39(19), 2012.

Böning, C.W., Behrens, E., Biastoch, A., Getzlaff, K., and Bamber, J.L.: Emerging impact of Greenland meltwater on deepwater formation in the North Atlantic Ocean. Nature Geoscience, 97(7), 523, 2016.

Brossier, C.L., Léger, L., Giordani, H.,Beuvier, J., Bouin, M.N., Ducrocq, W., and Fourrié, N.: Dense water formation in the north-western Mediterranean area during HyMeX-SOP2 in 1/36° ocean simulations: Ocean-atmosphere coupling impact. Journal of Geophysical Research: Oceans, 122(7), 5749-5773, 2017.

Bryden, H.L., Longworth, H.R., and Cunningham, S.A.: Slowing of the Atlantic meridional overturning circulation at 25°N. Nature, 438(7068), 655, 2005.

https://doi.org/10.5194/gmd-2020-111
Preprint. Discussion started: 30 April 2020

Geoscientific Model Development Discussions

Chanut, J., Barnier, B., Large, W., Debreu, L., Penduff, T., Molines, J.M., and Mathiot, P.: Mesoscale eddies in the Labrador Sea and their contribution to convection and restratification. Journal of Physical Oceanography, 28(8), 1617-1643, 2008.

Chassignet, E.P. and Xu, X.: Impact of horizontal resolution (1/12 to 1/50) on Gulf Stream separation, penetration, and variability. Journal of Physical Oceanography, 47(8), 1999-2021, 2017.

Courtois, P., Hu, X., Pennelly, C., Spence, P., and Myers, P.G.: Mixed layer depth calculation in deep convection regions in ocean numerical models. Ocean Modelling, 120, 60-78, 2017.

Cuny, J., Rhines, P.B., and Kwok, R.,: Davis Strait volume, freshwater and heat fluxes. Deep Sea Research Part I: Oceanographic Research Papers, 52.3, 519-542, 2005.

Curry, B., Lee, C.M., and Petrie, B.: Volume, freshwater, and heat fluxes through Davis Strait, 2004-05. Journal of Physical Oceanography, 41(3), 429-436, 2011.

Curry, B., Lee, C.M., Petrie, B., Moritz, R.E. and Kwok, R.: Multiyear volume, liquid freshwater, and sea ice transports through Davis Strait, 2004-10. Journal of Physical Oceanography, 44(4), 1244-1266, 2014.

Dai, A., Qian, T., Trenberth, K.E., and Milliman, J.D.: Changes in continental freshwater discharge from 1948 to 2004. Journal of Climate, 22(10), 2773-2792, 2009.

Debreu, L., Vouland, C., and Blayo, E.: AGRIF: Adaptive grid refinement in Fortran. Computers and Geosciences, 34(1), 8-13, 2008.

Dussin, R., Barnier, B., and Brodeau, L.: The making of Drakkar forcing set DFS5, Grenoble, France: LGGE, 2016.

Ferry, N., Parent, L., Garric, G., Barnier, B., and Jourdain, N.C.: Mercator global eddy permitting ocean reanalysis GLORYS1V1: Description and results. Mercator-Ocean Quarterly Newsletter, 36, 15-27, 2010.

Fischer, J., Visbek, M., Zantopp, R., Nunes, N.: Interannual to decadal variability of outflow from the Labrador Sea. Geophysical Research Letters, 37(24), 2010.

Fichefet, T., and Maqueda, M.A.M.: Sensitivity of a global sea ice model to the treatment of ice thermodynamics and dynamics. Journal of Geophysical Research: Oceans, 102(C6), 12609-12646, 1997.

https://doi.org/10.5194/gmd-2020-111
Preprint. Discussion started: 30 April 2020

Geoscientific Model Development Discussions
Open Access
EGU

Frajka-Williams, E., Rhines, P.B., and Eriksen, C.C.: Horizontal stratification during deep convection in the Labrador Sea. Journal of Physical Oceanography, 44(1), 220-228, 2014.

Fratantoni, P.S. and Pickart, R.S.: The Western North Atlantic Shelfbreak Current System in Summer. Journal of Physical Oceanography, 37(10), 2509-2533, 2007.

Fresnay, S., Ponte, A.L., Le Gentil, S., Le Sommer, J.: Reconstruction of the 3-D dynamics from surface variable in a high-resolution simulation of the North Atlantic. Journal of Geophysical Research: Oceans, 123(3), 1612-1630, 2018.

Garcia-Quintana, Y., Courtois, P., Hu, X., Pennelly, C., Kieke, D., and Myers, P.G.: Sensitivity of Labrador Sea Water formation to changes in model resolution, atmospheric forcing, and freshwater input. Journal of Geophysical Research: Oceans, 124(3), 2126-2152, 2019.

Gelderloos, R., Katsman, C.A. and Drijfhout, S.S.: Assessing the roles of three eddy types in restratifying the Labrador Sea after deep convection. Journal of Physical Oceanography, 41(11), 2102-2119, 2011.

Gordon, A.L., Visbeck, M., and Comiso, J.C.: A possible link between the Weddell Polynya and the Southern Annular Mode. Journal of Climate, 20(11), 2558-2571, 2007.

Hansen, B., and Østerhus, S.: North Atlantic-Nordic Seas exchanges. Progress in Oceanography, 45(2), 109-208, 2000.

Holdsworth, A.M., and Myers, P.G.: The influence of high-frequency atmospheric forcing on the circulation and deep convection of the Labrador Sea. Journal of Climate, 28(12), 4980-4996, 2015.

Holte, J., and Talley, L.: A new algorithm for finding mixed layer depths with applications to Argo data and Subantarctic Mode Water formation. Journal of Atmospheric and Oceanic Technology, 26(9), 1920-1939, 2009.

Kieke, D., Klein, B., Stramma, L., Rhein, M., and Koltermann, K.P.: Variability and propagation of Labrador Sea Water in the southern subpolar North Atlantic. Deep Sea Research Part I: Oceanographic Research Papers, 56(10), 1656-1674, 2009.

Lab Sea Group: The Labrador Sea deep convection experiment. Bulletin of the American Meteorological Society, 79(10), 2033-2058, 1998.

https://doi.org/10.5194/gmd-2020-111
Preprint. Discussion started: 30 April 2020

Lazier, J., Hendry, R., Clarke, A., Yashayaev, I., and Rhines, P.: Convection and restratification in the Labrador Sea, 1990-2000. Deep Sea Research Part I: Oceanographic Research Papers, 49(10), 1819-1835, 2002.

Lazier, J.R.N., and Wright, D.G.: Annual velocity variations in the Labrador Current, Journal of Physical Oceanography, 23(4), 659-678, 1993.

Lilly, J.M., Rhines, P.B., Schott, F., Lavender, K., Lazier, J., Send, U., and D'Asaro, E.: Observations of the Labrador Sea eddy field. Progress in Oceanography, 59(1), 75-176, 2003.

Madec, G.: Note du Pôle de modélisation. Institut Pierre-Simon Laplace (IPSL), France, No 27, ISSN No 1288-1619, 2008.

Marshall, J. and Schott, F.: Open-ocean convection: Observations, theory, and models. Reviews of Geophysics, 37(1), 1-64, 1999.

Marson, J.M., Myers, P.G., Hu, X., and Le Sommer, J.: Using vertically integrated ocean fields to characterize Greenland Icebergs' distribution and lifetime. Geophysical Research Letters, 45(9), 4208-4217, 2018.

Marzocchi, A., Hurshi, J.J.M., Holiday, N.P., Cunningham, S.A., Blaker, A.T., and Coward, A.C.: The North Atlantic subpolar circulation in an eddy-resolving global ocean model. Journal of Marine Systems, 142, 126-143, 2015..

McGeehan, I. and Maslowski, W.: Impact of shelf-basin freshwater transport on deep convection in the western Labrador Sea. Journal of Physical Oceanography, 41(11), 2187-2210, 2011.

Müller, V., Kieke, D., Myers, P.G., Pennelly, C., and Mertens, C.: Temperature flux carried by individual eddies across 47° in the Atlantic Ocean. Journal of Geophysical Research: Oceans, 122(3), 2441-2464, 2017.

Müller, V., Kieke, D., Myers, P.G., Pennelly, C., Steinfeldt, R., and Stendardo, I.: Heat and freshwater transport by mesoscale eddies in the southern subpolar North Atlantic. Journal of Geophysical Research: Oceans, 124(8), 5565-5585, 2019.

Myers, P.: Impact of freshwater from the Canadian Arctic Archipelago on Labrador Sea water formation. Geophysical Research Letters, 32(6), 2005.

https://doi.org/10.5194/gmd-2020-111
Preprint. Discussion started: 30 April 2020

Pennelly, C.: A 1/60 degree NEMO configuration within the Labrador Sea: LAB60, Zenodo, http://doi.org/10.5281/zenodo.3762748, 2020.

Pennelly, C. Hu, X., and Myers, P.G.: Cross-isobath freshwater exchange within the North Atlantic Subpolar Gyre. Journal of Geophysical Research: Oceans, 124(10), 6831-6853, 2019.

Rattan, S., Myers, P.G., Trequier, A.M., Theetten, S., Biastoch, A., and Böning, C. Towards an understanding of Labrador Sea salinity drift in eddy-permitting simulations. Ocean Modelling, 35(102), 77-88, 2010.

Rieck, J.K., Böning, C.W., and Getzlaff, K.: The nature of eddy kinetic energy in the Labrador Sea: Different types of mesoscale eddies, their temporal variability, and impact on deep convection. Journal of Physical Oceanography, 49(8), 2075-2094, 2019.

Schmidt, S. and Send, U.: Origin and composition of seasonal Labrador Sea freshwater. Journal of Physical Oceanography, 37(6), 1445-1454, 2007.

Schulze, L.M., Pickart, R.S., and Moore, G.W.K.: Atmospheric forcing during active convection in the Labrador Sea and its impact on mixed-layer-depths. Journal of Geophysical Research: Oceans, 121(9), 6978-6992, 2016.

Smith, G.C., Roy, F., Mann, P., Dupont, F., Brasnett, B., Lemieux, J.F., Laroche, S., and Bélair, S.: A new atmospheric dataset for forcing ice-ocean models: Evaluation of reforecasts using the Canadian global deterministic prediction system. Quarterly Journal of the Royal Meteorological Society, 140(680), 881-894, 2014.

Straneo, F.: Heat and freshwater transport through the central Labrador Sea. Journal of Physical Oceanography, 36(4), 606-628, 2006.

Straneo, F. and Saucier, F.: The arctic-subarctic exchange through Hudson Strait. Arctic-Subarctic Ocean Fluxes, Springer, Dordrecht, 249-261, 2008.

De Steur, L., Hansen, E., Gerdes, R., Karcher, M., Fahrbach, E., Holfort, J.: Freshwater fluxes in the East Greenland Current: A decade of observations. Geophysical Research Letters, 36(23), 2009.

Tréquier, A.M., Theetten, S., Chassignet, E.P., Penduff, T., Smith, R., Talley, L., Beismann, J.O., and Böning, C.: The North Atlantic subpolar gyre in four high-resolution models. Journal of Physical Oceanography, 35(5), 757-774, 2005.

https://doi.org/10.5194/gmd-2020-111
Preprint. Discussion started: 30 April 2020

Geoscientific Model Development Discussions
Open Access
EGU

Yashayaev, I. and Loder, J.W.: Recurrent replenishment of Labrador Sea Water and associated decadal-scale variability. Journal of Geophysical Research: Oceans, 121(11), 8095-8814, 2016.

Yashayaev, I.: Hydrographic changes in the Labrador Sea, 1960-2005. Progress in Oceanography, 73(3-4), 242-276, 2007.

Whiteworth, T. and Orsi, A.H.: Antarctic Bottom Water production and export by tides in the Ross Sea. Geophysical Research Letters 33(12), 2006.

Zalesak, S.T.: Fully multidimensional flux-corrected transport algorithms for fluids. Journal of computational physics, 31(3), 335-362, 1979.

Table 1: Domain settings for the ANHA4 parent domain, SPG12 and LAB60 nested domains. Other settings which are invariant to the domain are shown in Table 2.

Setting	ANHA4	SPG12	LAB60
Horz. Resolution	1/4°	1/12°	1/60°
X points	544	724	1179
Y points	800	694	2659
Timestep [s]	720	240	48
Horiz. Eddy Viscosity [m^4 s^{-1}]	1.5x10^11	1.5x10^10	3.5x10^8
Horiz. Eddy Diffusivity [m^2 s^{-1}]	300	50	20
Lateral Slip Conditions	Free slip	Free slip	No slip

Table 2: Model configuration settings which are identical between all three domains. **Bold** values indicate values which were changed when we migrated LAB60 from the Graham cluster to Niagara.

https://doi.org/10.5194/gmd-2020-111
Preprint. Discussion started: 30 April 2020

Geoscientific Model Development Discussions
Open Access

Configuration Setting	Value
Vertical grid	75 geopotential levels
Sea-ice model	LIM 2
Bulk formula	CORE
Liquid discharge	Dia et al. (2009) + Bamber (2012: Greenland)
Solid discharge	Input as liquid
Surface Restoring	None
Initial conditions	Glorys1v1 (T,S,U,V,SSH,ice)
Open boundary conditions	Glorys1v1 (T,S,U,V,ice)
Lateral momentum	Bilaplacian operator
Lateral diffusion	Laplacian operator
Vertical eddy viscosity	1x10^-4 m^2 s^{-1}
Vertical eddy diffusivity	1x10^-5 m^2 s^{-1}
Mixed layer scheme	Holte and Talley (2009)
Bottom friction	Nonlinear
Hydrostatic approximation	Yes
Passive tracers	Three (see Figure 2)
CPU requested	672 (**3000**), Broadwell 2.1 GHz (Skylake 2.4 GHz)
Time to complete 1 year	Approximately 700 (**200**) hours
Initialization date	January 1st, 2002

Figures

https://doi.org/10.5194/gmd-2020-111
Preprint. Discussion started: 30 April 2020

Geoscientific Model Development
Discussions
Open Access

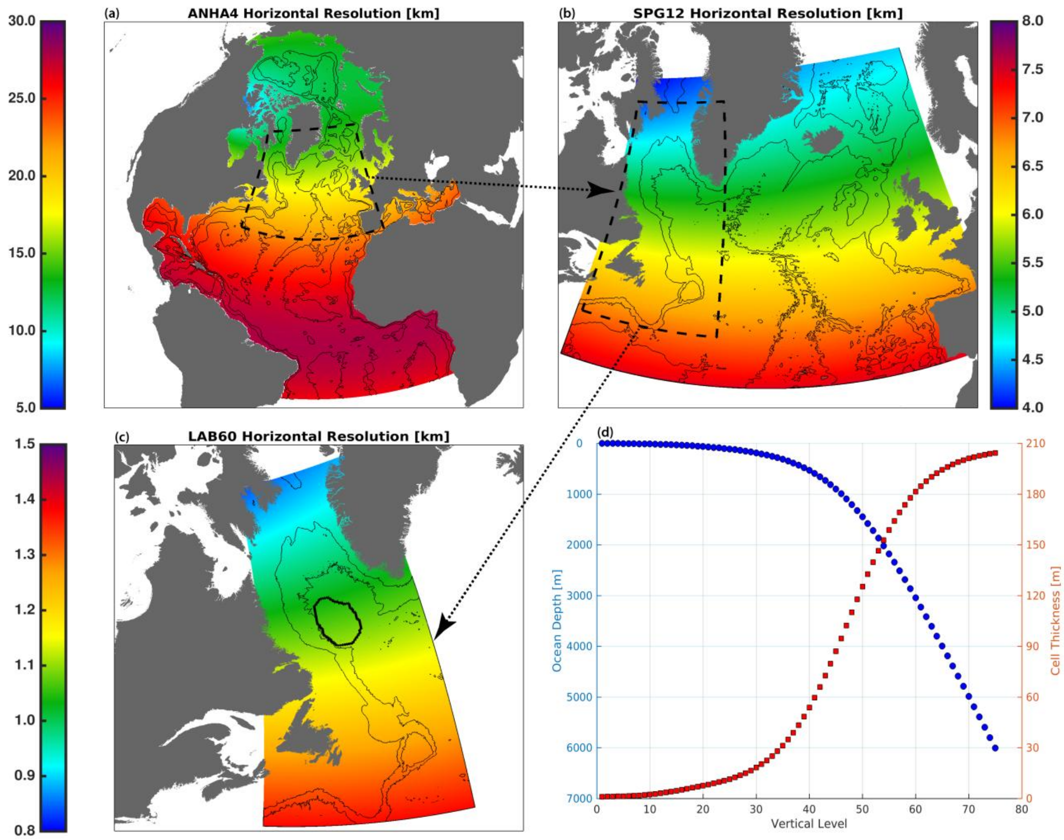

Figure 1: Domain setup for the (a) ANHA4 parent domain, (b) the SPG12 nest, and (c) the LAB60 nest. Horizontal grid resolution, in km, is identified by color. All domains share identical vertical grid structure (d). The black contour in (c) identifies a region of interest where calculations of LSW's density and thickness, as well as the depth of the mixed layer are performed. The 1000m, 3000m, and 5000m isobaths are shown via the thin black contours.

https://doi.org/10.5194/gmd-2020-111
Preprint. Discussion started: 30 April 2020

Geoscientific Model Development
Discussions

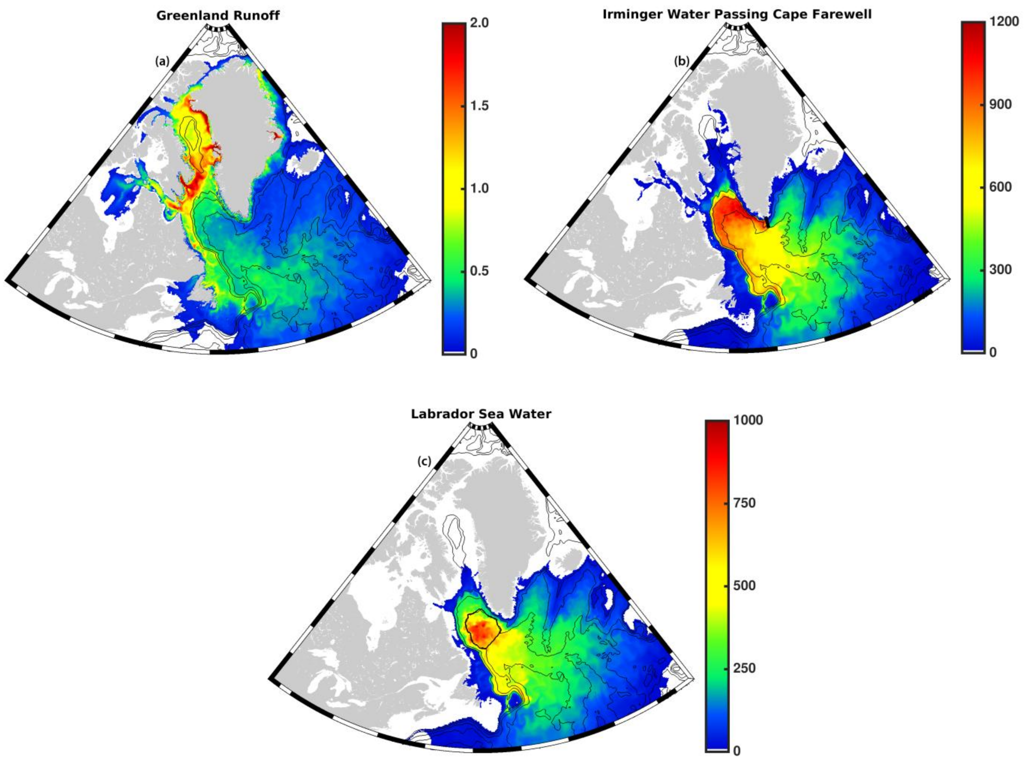

Figure 2: The three passive tracers used within our LAB60 simulation with source regions indicated by thick black lines: (a) Greenland runoff, (b) Irminger Water (T > 3.5°C, S > 34.88) which flows west past Cape Farwell, and (c) Labrador Sea Water (σ>27.68 kg m^{-3}) produced each convective season. Images are from the simulation date 1 Jan 2010. Bathymetric contours are every 1000m. Units are the thickness, in meters, of the tracer. Note: as all three domains are included in this figure, spatial resolution changes within each figure- see Hudson Strait for a clear example.

https://doi.org/10.5194/gmd-2020-111
Preprint. Discussion started: 30 April 2020

Geoscientific Model Development
Discussions

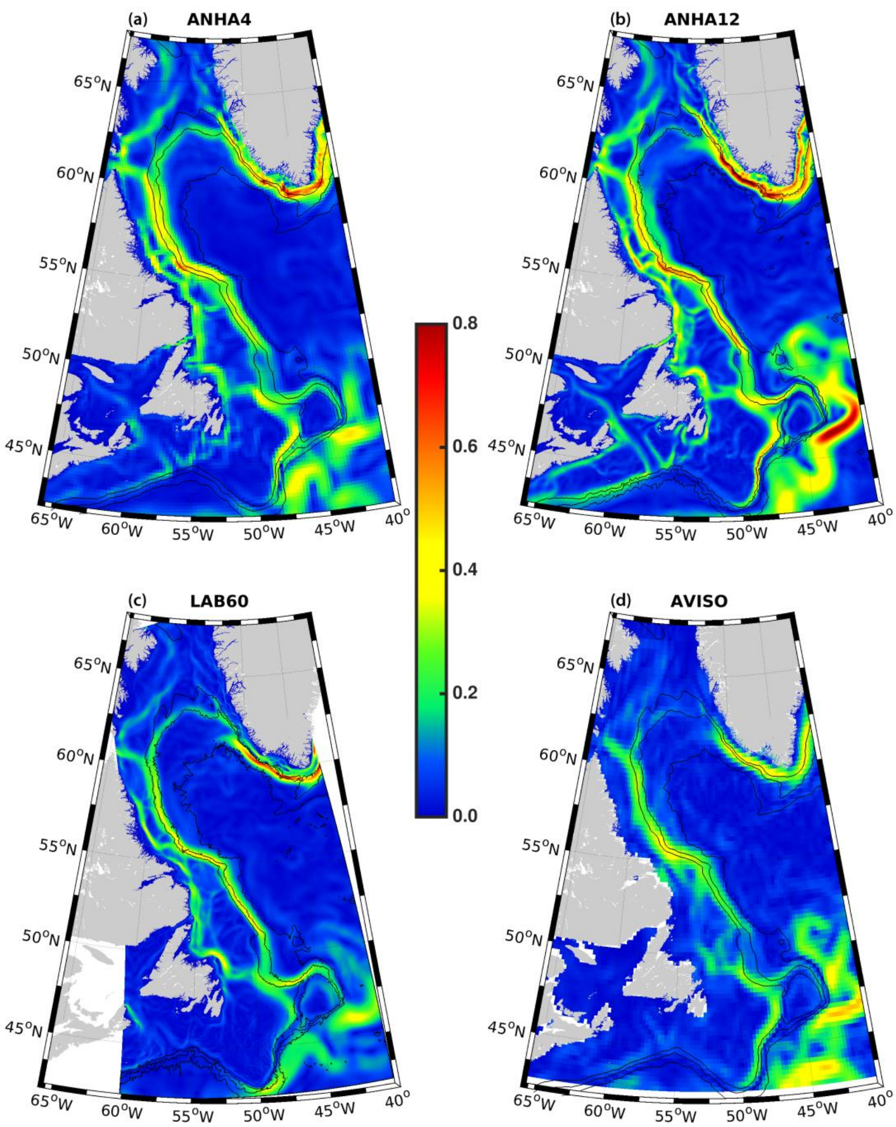

551

552 Figure 3: Average speed (m s^{-1}: 2004-2010) for the (a) ANHA4, (b) ANHA12, (c) and LAB60

553 simulations, as well as (d) derived from AVISO observations. The 1000, 2000, and 3000m

554 isobaths are shown by the black contour lines.

555

https://doi.org/10.5194/gmd-2020-111
Preprint. Discussion started: 30 April 2020

Geoscientific Model Development Discussions

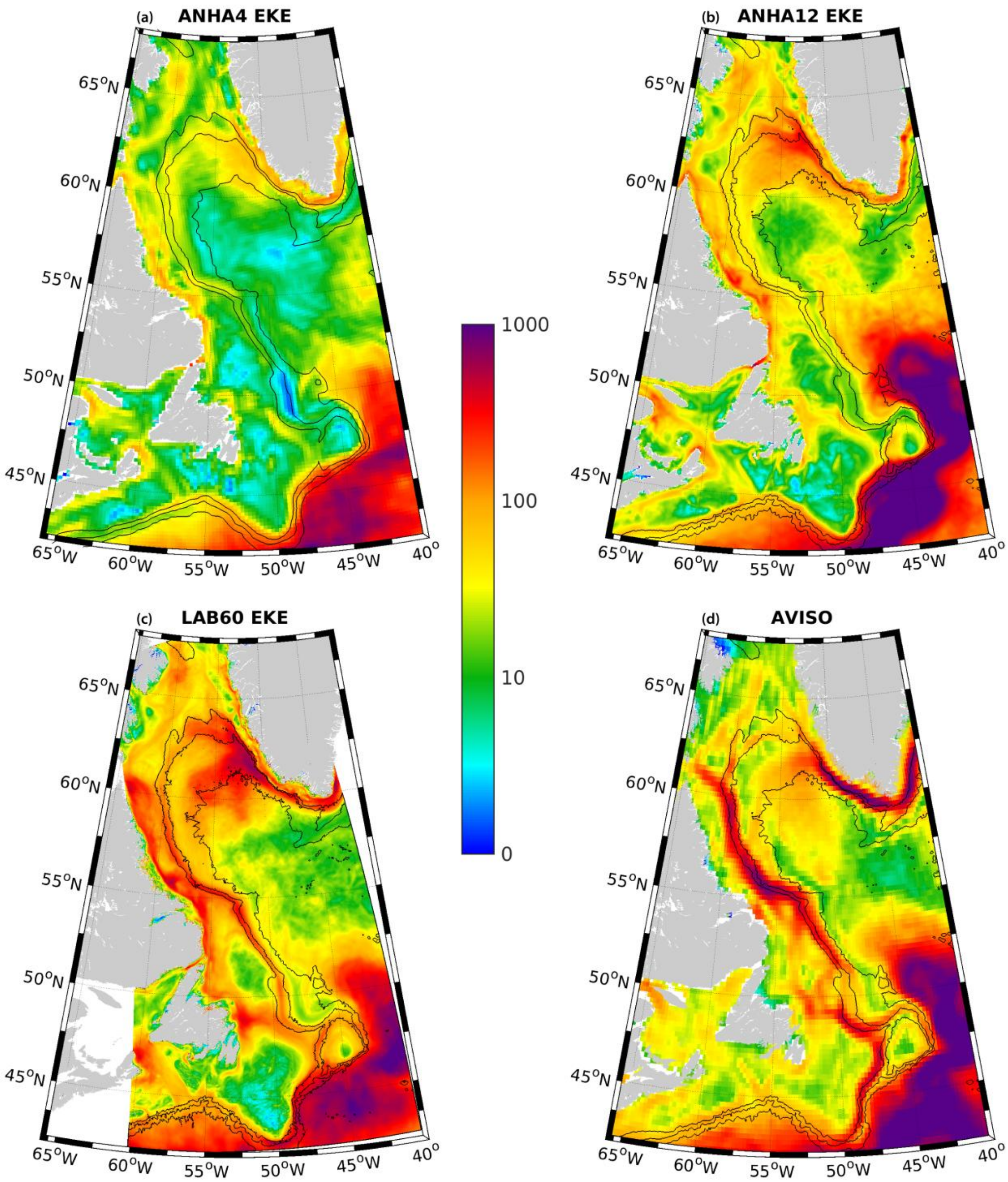

Figure 4: Eddy Kinetic Energy derived from (a) ANHA4, (b) ANHA12, and (c) our LAB60 simulation, from 2004 to 2010. Observations via AVISO are identified in (d). Units are in $cm^2 s^{-2}$. The 1000m, 2000m, and 3000m isobaths are shown by the black contour lines. Note: a log scale was used for clarity.

https://doi.org/10.5194/gmd-2020-111
Preprint. Discussion started: 30 April 2020

Geoscientific Model Development
Discussions

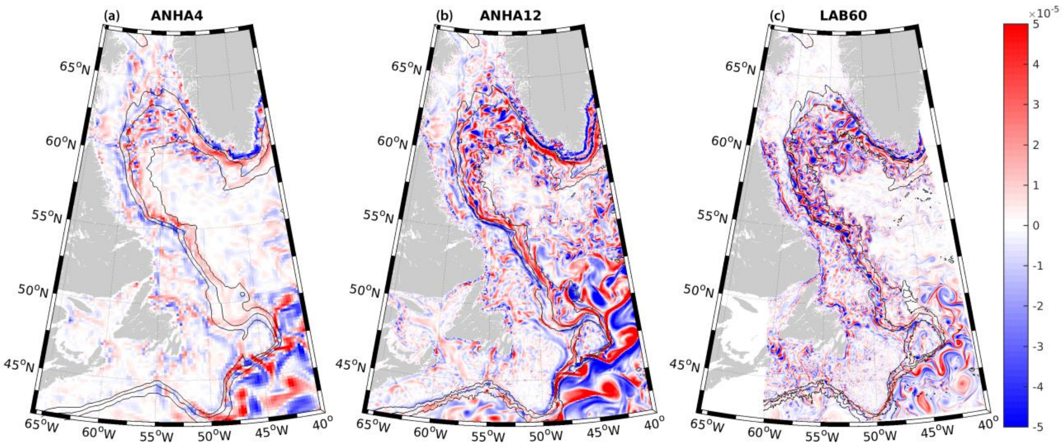

Figure 5: Relative vorticity as simulated by (a) ANHA4, (b) ANHA12, and (c) LAB60 on 16 March 2008. Units are in s^{-1}. The 1000m, 2000m, and 3000m isobaths are shown by the black contour lines.

https://doi.org/10.5194/gmd-2020-111
Preprint. Discussion started: 30 April 2020

Geoscientific Model Development
Discussions
Open Access
EGU

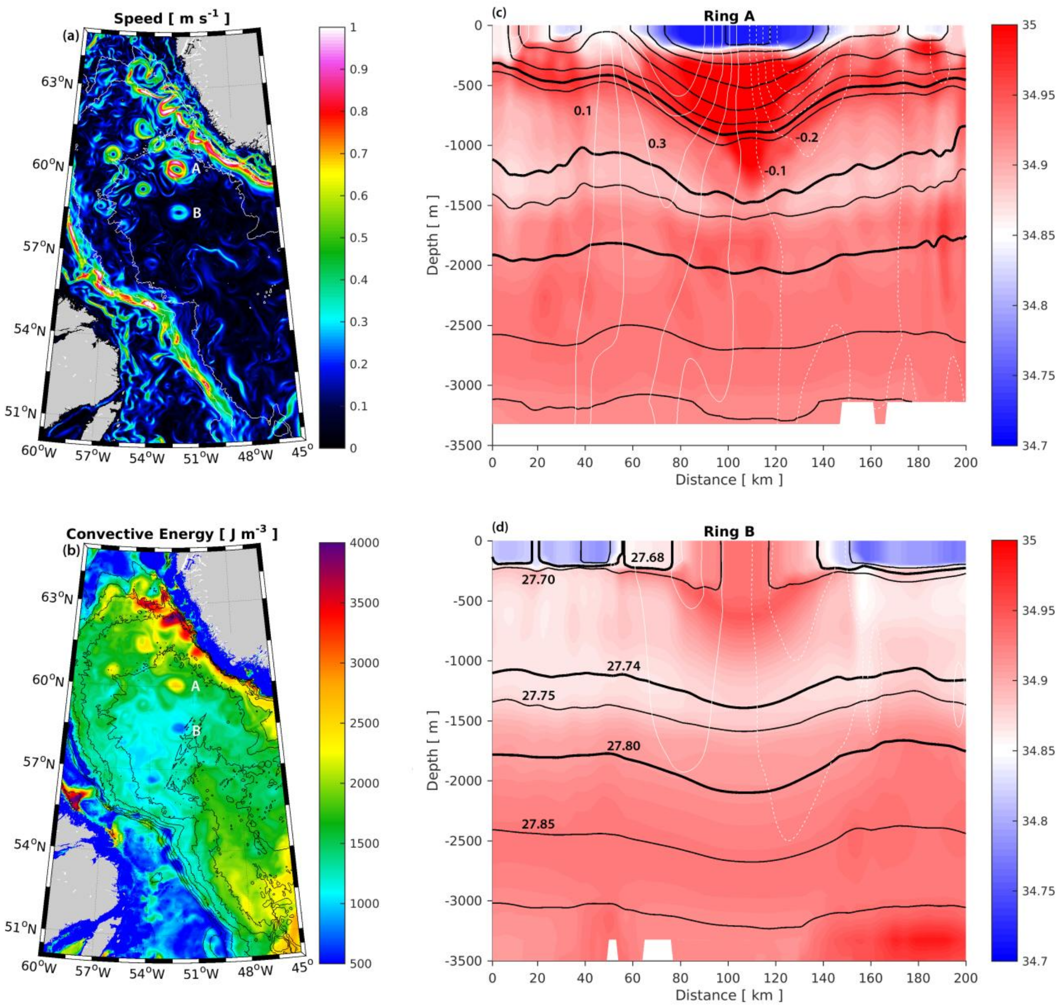

Figure 6: LAB60 snapshot (17 Jan 2003) of the speed (a) and stratification (b) within the Labrador Sea. Two Irminger Rings are identified by their age with letters: Ring A is a young Irminger Ring, while Ring B is comparatively older. An east-west cross section through each of these Irminger Rings is shown in (c) and (d) where colors indicate salinity, black contours indicate potential density using a contour interval of 0.05 kg m^{-3}, and white contours indicate meridional velocity where southern flow is dashed and northern flow is solid, using a contour interval of 0.1 m s^{-1}. Thick black contours indicate the potential density classification of Upper Labrador Sea Water (27.68-27.74 kg m^{-3}) and Classical Labrador Sea Water (27.74-27.80 kg m^{-3}).

https://doi.org/10.5194/gmd-2020-111
Preprint. Discussion started: 30 April 2020

Geoscientific Model Development Discussions
Open Access

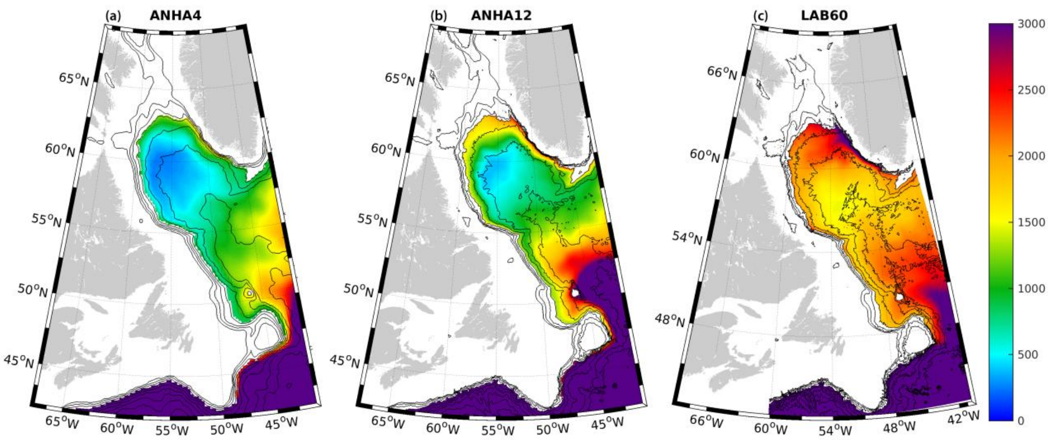

Figure 7: The convective energy, the strength of stratification down to a reference depth of 2000m, is shown for (a) ANHA4, (b) ANHA12, and (c) LAB60. Convective energy was averaged from 2004 through 2010. Values where the depth of the seafloor was less than 2000m were removed to preserve clarity. Units are in J m^{-3}. Bathymeric contours (black lines) are shown every 500m.

https://doi.org/10.5194/gmd-2020-111
Preprint. Discussion started: 30 April 2020

Geoscientific Model Development
Discussions
Open Access

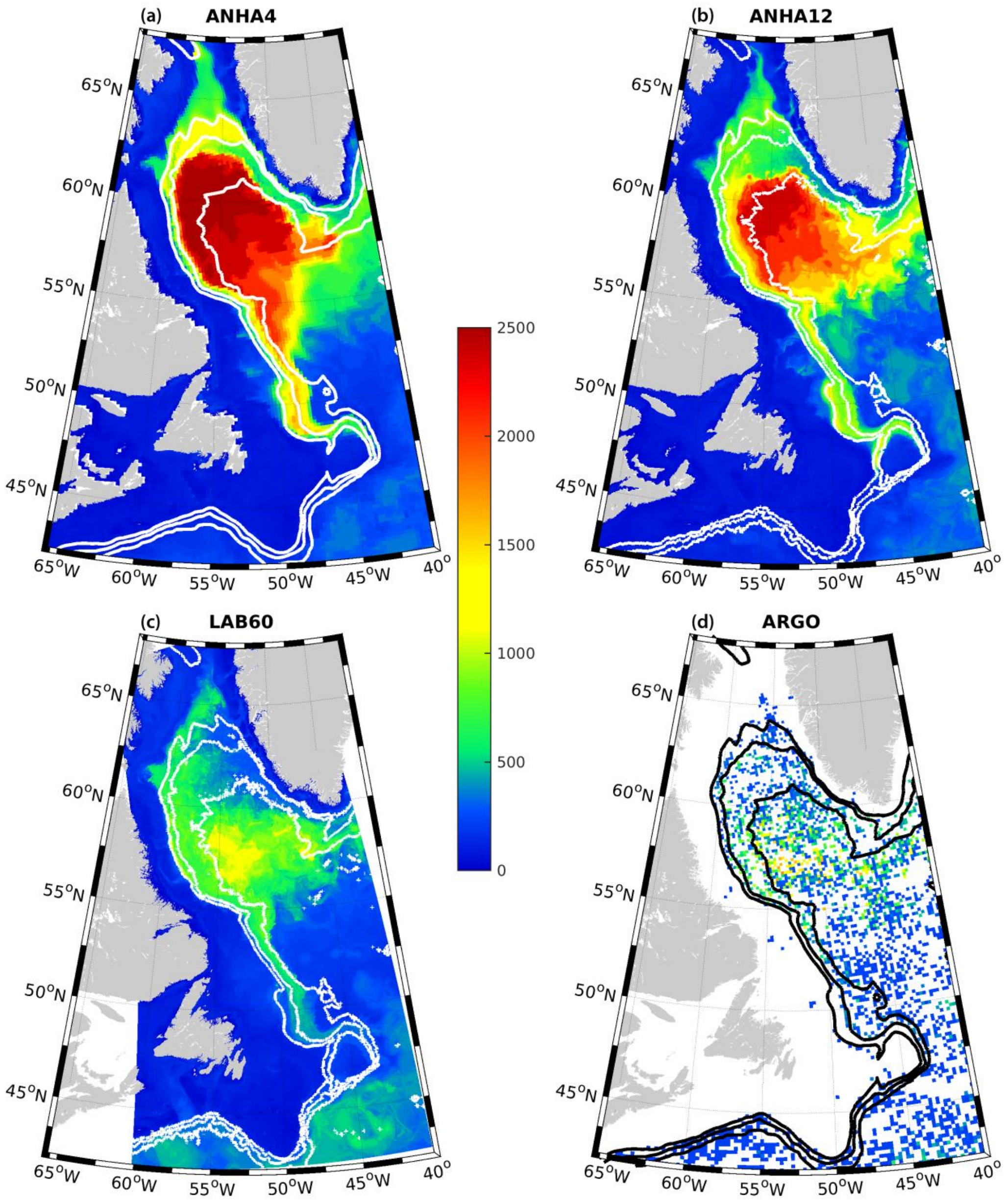

Figure 8: Maximum mixed layer depth for (a) ANHA4, (b) ANHA12, (c) LAB60, as well as (d) ARGO observations, where available, from 2004 through the end of 2010. For clarity, the ARGO data were placed on the same grid as ANHA4. Units are in meters. The 1000m, 2000m, and 3000m isobaths are shown via the white and black contours

https://doi.org/10.5194/gmd-2020-111
Preprint. Discussion started: 30 April 2020

Geoscientific Model Development
Discussions
Open Access
EGU

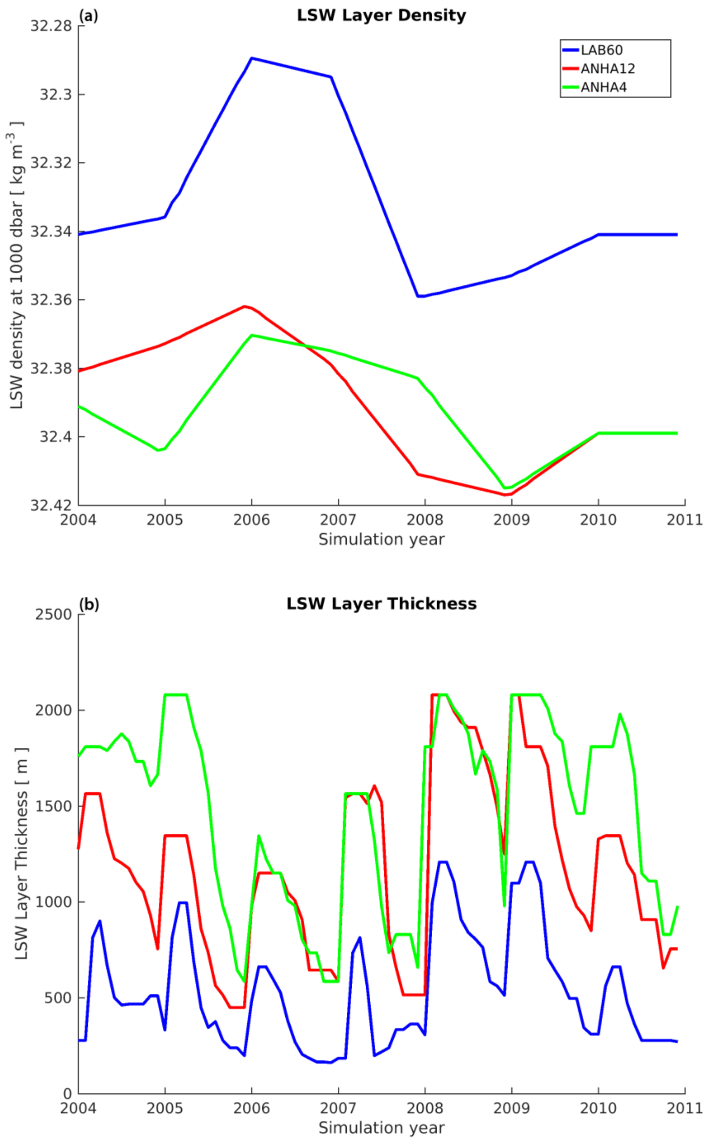

Figure 9: Labrador Sea Water (LSW) density (a) and thickness (b) for the LAB60, ANHA12, and ANHA4 configurations. LSW density was determined from the thickest layer where a 0.001 kg m^{-3} change in density occurred. The LSW layer thickness was then calculated between this density and one which was 0.02 kg m^{-3} lighter. Values were taken from the white region in Fig 1c.